Comparison of Rate of Change between Bruch's Membrane Opening Minimum Rim Width and Retinal Nerve Fiber Layer in Eyes Showing Optic Disc Hemorrhage

HYUN-KYUNG CHO AND CHANGWON KEE

• PURPOSE: To investigate and compare the longitudinal rate of change of Bruch's membrane opening minimum rim width (BMO-MRW) and peripapillary retinal nerve fiber layer (RNFL) thickness in eyes showing optic disc hemorrhage(DH).

• DESIGN: Observational case series.

• METHODS: A total of 82 subjects(82 eyes) showing DH who had undergone more than five reliable spectral-domain optical coherence tomography (OCT) tests were included. BMO-MRW and RNFL were measured with OCT at 3-month intervals. The rates of change in global and each Garway-Heath sector were calculated with a linear mixed-effects model after adjusting for age, sex, and BMO area.

• RESULTS: The mean follow-up period was 21.57 ± 7.88 months with a mean number of 7.88 ± 2.39 OCT tests. Baseline demographics were age (58.37 ± 10.65 y); 46.3% were female; and the mean deviation was −4.41 ± 5.04 dB. The global rate of change in BMO-MRW was −3.507 ± 0.675 μm/y and in −1.404 ± 0.208 μm/y in RNFL. The rate of change was the greatest in the inferotemporal sector, which was −9.141 ± 1.254 μm/y in BMO-MRW and −4.204 ± 0.490 μm/y in the RNFL. The rate of change was significantly greater in BMO-MRW than in the RNFL in all sectors, except for the nasal sector ($P < .05$). Percentage of reduction was significantly greater in BMO-MRW than in RNFL in the inferotemporal and superotemporal sectors ($P < .05$).

• CONCLUSIONS: BMO-MRW showed a significantly greater rate of change than RNFL in eyes showing DH, especially in the inferotemporal and superotemporal sectors in percentage of reduction. Thus, it may be more advantageous to detect glaucomatous progression earlier in BMO-MRW than in the RNFL in eyes showing DH that are more likely to progress. (Am J Ophthalmol 2020;217:27–37. © 2020 Elsevier Inc. All rights reserved.)

AJO.com Supplemental Material available at AJO.com.

Accepted for publication Mar 31, 2020.

From the Department of Ophthalmology (H-K.C.), Gyeongsang National University Changwon Hospital, Gyeongsang National University, School of Medicine, Changwon, Gyeongsangnam-do, 51472, Republic of Korea; Institute of Health Sciences (H-K.C.), School of Medicine, Gyeongsang National University, Jinju, Republic of Korea; and the Department of Ophthalmology (C.K.), Samsung Medical Center, Sungkyunkwan University School of Medicine, Seoul, Republic of Korea.

Inquiries to Hyun-kyung Cho, Department of Ophthalmology, Gyeongsang National University Changwon Hospital, Gyeongsang National University, School of Medicine, 11 Samjeongja-ro, Seongsan-gu, Changwon, Gyeongsangnam-do, 51472, Republic of Korea; e-mails: chohk@gnu.ac.kr; kanojo99@hanmail.net

GLAUCOMA IS CAUSED BY THE INJURY OF RETINAL ganglion cells (RGC) and axons of RGCs, bringing about a loss of the retinal nerve fiber layer (RNFL) along with the neuroretinal rim (NRR) that can result in visual field damage.[1] Optic disc hemorrhage (DH) has been an issue since its initial description by Lee and associates[2] because DH is recognized to be strongly associated with the development of glaucoma and its progression.[2–13]

The involvement of DH in the progression of glaucoma has been extensively described.[2,3,7,8,11,13–19] In the beginning, DH was regarded as a preceding event for glaucomatous injury as the discovery of DH was accompanied by a diagnosis of glaucoma or its progression.[2,3,7,8,11,13,14,16–19] However, recently, it has been proposed that DH may not be a separate episode resulting in glaucomatous progression but instead a consequence of glaucomatous alterations.[2,4,20,21] DH is frequently followed by a progressive decline of the RNFL, as shown by optical coherence tomography (OCT).[22–31] Detectable structural changes precede functional visual field defects in glaucoma progression.[32–34] Therefore, the structural parameters obtained by OCT may be more beneficial in detecting early progression than a visual field test.

Recently, a new parameter, Bruch's membrane opening minimum rim width (BMO-MRW), has been presented in the estimation of discs.[26–30] The shortest distance between the inner opening of the BMO and the internal limiting membrane is measured for BMO-MRW (Figure 1, B and C). BMO-MRW offers reliable borders of discs and more correct assessment of the NRR than conventional ophthalmic examination.[26–28,31] The latest studies have likewise revealed that BMO-MRW provides a better diagnosis of glaucoma than existing neural rim

0002-9394/$36.00
https://doi.org/10.1016/j.ajo.2020.03.051

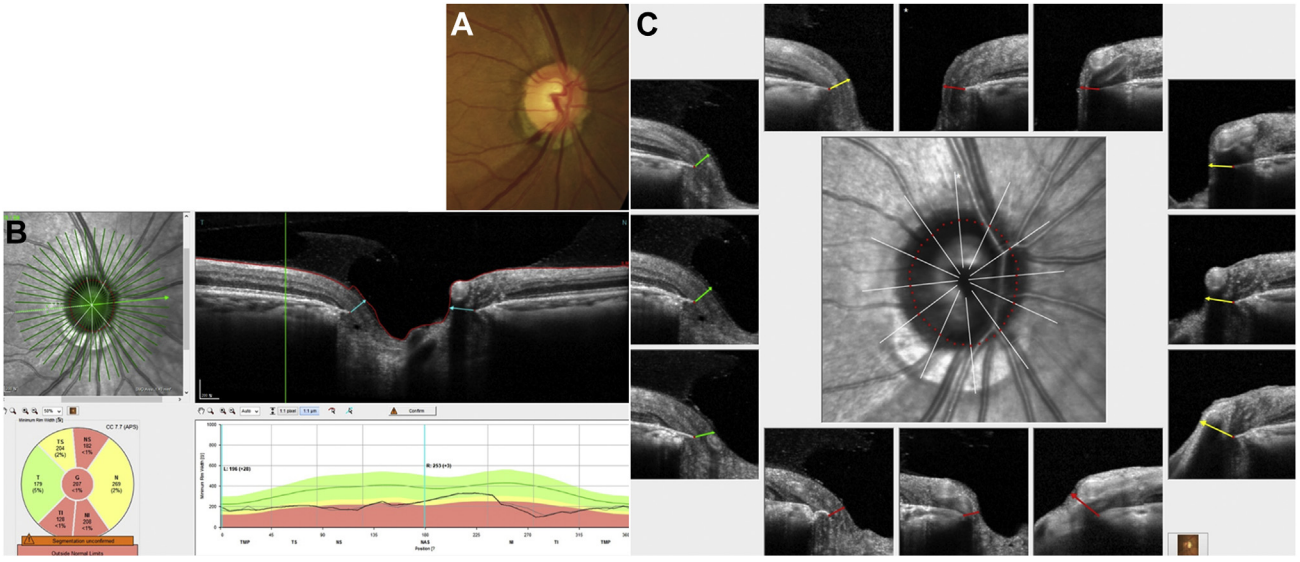

FIGURE 1. BMO-MRW. (A) Photograph of the optic disc shows optic disc hemorrhage for reference. (B) BMO-MRW is a newly proposed parameter in the assessment of the optic disc. The minimum length is measured from the BMO (red dot) to the internal limiting membrane (red line). The global BMO-MRW and 6 Garway-Heath sectors are shown. The FoBMO axis, which is the axis between the fovea and the center of the BMO, was applied in sectoral analysis. This can lead to a more accurate sectoral analysis, considering the cyclotorsion of individual eyes. (C) BMO margin of the optic disc and BMO-MRW measurement scan images from 12 directions are shown in this BMO overview. BMO-MRW = Bruch's membrane opening-minimum rim width; FoBMO = Foveo-BMO.

parameters.[28–30] BMO-MRW showed a stronger structure-function relationship than other conventional peripapillary RNFL and confocal scanning laser ophthalmoscope-based parameters in glaucoma.[30,31,35,36] The present authors previously reported a discrepancy between BMO-MRW and RNFL color-coded classification. The structural changes are minimal in early glaucomatous stage and different structural tests may not show consistent findings. These authors found that BMO-MRW could yield a normal classification, whereas the RNFL showed abnormal classifications in cases of large discs and myopia, which suggest clinically useful examples of BMO-MRW.[37]

A longitudinal study regarding the rate of change (ROC) of the new BMO-MRW parameter has not yet been conducted. The effect of normal aging on the ROC of BMO-MRW was investigated by Vianna and associates.[38] Because the study was conducted in Canada, mainly whites were included. Another study compared the ROC of BMO-MRW in different populations of European and African descent[39] and found that neither European nor African descent was a significant factor in evaluating changes in BMO-MRW in eyes with suspected glaucoma. However, the ROC of BMO-MRW in Asians has not yet been studied. Moreover, it has not been investigated in patients showing DH in any ethnicity to our knowledge. DH is a common and important glaucomatous phenomenon, considering the strong association with glaucoma progression. The ROC is particularly important in determining the intensity of glaucoma treatment for these potentially fast-progressing patients showing DH. Moreover, early detection of glaucomatous deterioration in these patients with DH is also highly important.

In this longitudinal observational case series, the ROC of BMO-MRW and the RNFL was investigated in patients showing DH. The ROC between these 2 parameters was also compared in a single ethnic group of Asians showing DH. The aim was to determine which parameter was more beneficial for the early detection of glaucomatous progression in patients with DH who are prone to progression.

SUBJECTS AND METHODS

THIS RETROSPECTIVE, LONGITUDINAL OBSERVATIONAL case series was carried out in keeping with the tenets of the Declaration of Helsinki. The current study was approved by the Institutional Review Board of Gyeongsang National University Changwon Hospital, Gyeongsang National University, School of Medicine. An exemption was granted from the requirement for informed consent because the present study was retrospective research.

• **SUBJECTS:** The subjects were assessed in the glaucoma clinic at Gyeongsang National University Changwon Hospital by a single glaucoma specialist (H-K.C.). When optic DH was observed on fundus photography and red-free photography, the subject was enrolled, and OCT data of

the immediately preceding visit 3 to 4 months earlier were included as a baseline. These previous data were included to eliminate the potential effect of the initial DH on the OCT parameters and also to eliminate any possible bias of the DH in the base line data in calculating the longitudinal ROC. Among 130 subjects showing optic DH, those who had undergone more than 5 reliable spectral-domain OCT sessions at 3-month intervals were included in the final analysis. A total of 82 eyes (82 subjects) showing optic DHs were included in the final analysis.

All subjects underwent standard ophthalmic examinations, including Spectralis spectral domain OCT (glaucoma module Premium edition; Heidelberg Engineering, Heidelberg, Germany) and standard automated perimetry (HFA model 840; Humphrey Instruments, San Leandro, California). BMO-MRW and the RNFL were measured with OCT at 3-month intervals. Those who had had both BMO-MRW and RNFL tests by OCT more than 5 times were included. In cases where both eyes met the criteria of inclusion, 1 eye was selected randomly.

Exclusion criteria included poor image scans due to eyelid blinking or bad fixation, history of any intraocular surgery except for uneventful phacoemulsification, history of optic neuropathies other than glaucoma or an acute angle closure crisis that could influence the thickness of the RNFL or BMO-MRW (eg, optic neuritis, acute ischemic optic neuritis), and retinal disease accompanied by retinal swelling or edema and subsequent RNFL or BMO-MRW swelling.

A reliable visual field test result had 3 criteria: fixation loss of <20%, a false positive rate of <15%, and a false negative rate of <15%.

• **OPTICAL COHERENCE TOMOGRAPHY:** The imaging scans were obtained by using Spectral-Domain OCT (Heidelberg Engineering) using the Glaucoma Module Premium Edition by an experienced technician. A total of 24 radial B-scans were obtained for BMO-MRW. For the peripapillary RNFL thickness, a scan circle diameter of 3.5 mm among 3 scan circle diameters (diameters of 3.5, 4.1, and 4.7 mm) was applied. Well-centered images with accurate segmentation of the retina and quality scores of more than 20 were used. OCT data were acquired and then analyzed in a specific individual axis (fovea Bruch's membrane opening axis [FoBMO axis]) of the eye, the axis between the BMO center and the fovea of macula, which could lead to more precise analysis of each sector concerning the cyclotorsion of individual eyes and more correct comparison of normative data than the conventional method of using simple clock-hour locations.[22]

• **STATISTICAL ANALYSIS:** To calculate the ROC, or progression rate as a regression coefficient, which is the slope of the values of each parameter (BMO-MRW and RNFL), a generalized linear mixed-effects model was used including a random intercept for the subjects. The ROCs in the global region and in each sector were estimated with the linear mixed-effects model after adjusting for age, sex, and BMO area. Comparison of the ROCs of BMO-MRW and the RNFL values in each sector and the global region was conducted with a *t*-test. Because the BMO-MRW and RNFL scales were different, as were the baseline values, the percentages of reduction in the progression rates and in the standardized coefficients were compared. The percentage of coefficient was calculated by setting the initial intercept to 100 at time = 0. Standardization was performed by calculating the mean as 0.0 and SD as 1.0. Statistical significance was indicated at a P value <.05. All statistical analyses were performed using SAS version 9.4 software (Cary, North Carolina).

TABLE 1. Baseline Characteristics of Included Subjects Showing Optic Disc Hemorrhage

Characteristics	Values
Number of subjects	82 eyes (82 subjects)
Mean ± SD age, y	58.37 ± 10.65
Females	38 (46.3%)
Family history of glaucoma	14 (17.1%)
Mean ± SD follow-up period, mo	21.57 ± 7.88
Mean ± SD number of OCT tests	7.88 ± 2.39
Mean ± SD quality score of RNFL	28.73 ± 3.34
Mean ± SD quality score of BMO-MRW	32.00 ± 3.17
FoBMO angle, degrees	−5.99 ± 3.63
Diagnosis	
NTG	57 (69.5%)
POAG	6 (7.3%)
PEX G	10 (12.2%)
PACG	3 (3.7%)
GS	6 (7.3%)
Mean ± SD spherical equivalent, D	−1.77 ± 2.53
Mean ± SD CCT, μm	540.32 ± 37.42
Mean ± SD baseline IOP, mm Hg	14.82 ± 3.21
Mean ± SD VFI, %	89.31 ± 14.79
Mean ± SD MD, dB	−4.41 ± 5.04
Mean ± SD PSD, dB	5.60 ± 4.12

BMO-MRW = Bruch's membrane opening-minimum rim width; CCT = central corneal thickness; D = diopters; FoBMO = fovea-Bruch's membrane opening; GS = glaucoma suspect; IOP = intraocular pressure; MD = mean deviation; NTG = normal tension glaucoma; OCT = optical coherence tomography; PACG = primary angle-closure glaucoma; PEX G = pseudoexfoliation glaucoma; POAG = primary open angle glaucoma; PSD = pattern standard deviation; RNFL = retinal nerve fiber layer; VFI = visual field index.

RESULTS

• **BASELINE CHARACTERISTICS:** From a total of 130 subjects, 82 eyes (82 subjects) were included in the final

TABLE 2. Progression Rate of BMO-MRW and RNFL per Year in Subjects with Optic Disc Hemorrhage

Outcome		Baseline value/Progression rate	Standard Error	95% CI		*P* Value
				Lower	Upper	
BMO area	Baseline, mm^2	2.34	0.68			
	Coefficient, mm2/y	−0.01106	0.006505	−0.02383	0.001721	0.0898
BMO-MRW global	Baseline, μm	203.04	57.97			
	Coefficient, μm/y	−3.507	0.675	−4.833	−2.181	**<0.0001**
RNFL global	Baseline, μm	82.88	15.37			
	Coefficient, μm/y	−1.404	0.208	−1.812	−0.996	**<0.0001**
BMO-MRW T	Baseline, μm	163.56	40.85			
	Coefficient, μm/y	−2.660	0.618	−3.874	−1.445	**<0.0001**
RNFL T	Baseline, μm	68.74	13.70			
	Coefficient, μm/y	−1.287	0.198	−1.676	−0.899	**<0.0001**
BMO-MRW TS	Baseline, μm	204.71	64.03			
	Coefficient, μm/y	−4.422	1.020	−6.425	−2.419	**<0.0001**
RNFL TS	Baseline, μm	107.83	34.73			
	Coefficient, μm/y	−1.353	0.420	−2.177	−0.529	**0.001**
BMO-MRW TI	Baseline, μm	184.62	74.21			
	Coefficient, μm/y	−9.141	1.254	−11.603	−6.679	**<0.0001**
RNFL TI	Baseline, μm	97.15	37.97			
	Coefficient, μm/y	−4.204	0.490	−5.165	−3.242	**<0.0001**
BMO-MRW N	Baseline, μm	221.34	69.67			
	Coefficient, μm/y	−1.618	0.786	−3.162	−0.075	**0.040**
RNFL N	Baseline, μm	68.61	15.10			
	Coefficient, μm/y	−0.517	0.223	−0.954	−0.080	**0.021**
BMO-MRW NS	Baseline, μm	230.21	78.87			
	Coefficient, μm/y	−3.573	0.978	−5.495	−1.651	**0.000**
RNFL NS	Baseline, μm	102.99	29.45			
	Coefficient, μm/y	−0.733	0.375	−1.469	0.003	0.051
BMO-MRW NI	Baseline, μm	233.12	79.23			
	Coefficient, μm/y	−4.807	1.122	−7.011	−2.602	**<0.0001**
RNFL NI	Baseline, μm	94.10	25.28			
	Coefficient, μm/y	−1.839	0.394	−2.612	−1.066	**<0.0001**

BMO-MRW = Bruch's membrane opening-minimum rim width; CI = confidence interval; G = global; N = nasal; NI = inferonasal; NS = superonasal; RNFL = retinal nerve fiber layer; T = temporal; TI = inferotemporal; TS = superotemporal;

P values were derived by generalized linear mixed-model including random intercept for subjects after adjusting for age, sex, and BMO area. Progression rate is calculated by coefficient by time per year (μm/y). Values in boldface indicate significant *P* values ($P < 0.05$) of the estimated slope (progression rate).

analysis. The mean follow-up period was 21.57 ± 7.88 months, and the mean number of OCT tests was 7.88 ± 2.39. The mean age of the subjects was 58.37 ± 10.65 years old. Of these subjects, 38 (46.3%) were women, 44 (53.7%) were men, and 14 (17.1%) of them had a family history of glaucoma. Diagnoses included normal-tension glaucoma (NTG) in 57 subjects (69.5%), primary open-angle glaucoma in 6 subjects (7.3%), pseudoexfoliative glaucoma in 10 subjects (12.2%), primary angle-closure glaucoma in 3 subjects (3.7%), and glaucoma suspected in 6 subjects (7.3%).

The mean spherical equivalent of all subjects was −1.77 ± 2.53 D. The mean baseline intraocular pressure was 14.82 ± 3.21 mm Hg, with a mean central corneal thickness of 540.32 ± 37.42 μm. The mean visual field index was 89.31 ± 14.79%. The mean deviation and pattern standard deviation were −4.41 ± 5.04 dB and 5.60 ± 4.12 dB, respectively (Table 1).

• **BASELINE AND RATE OF CHANGE IN BMO-MRW AND RNFL:** The mean baseline BMO area was 2.34 ± 0.68 mm^2 (Table 2). The mean baseline global BMO-MRW and RNFL were 203.04 ± 57.97 μm and 82.88 ± 15.37 μm, respectively (Table 2). The baseline values of the other sectors of BMO-MRW and RNFL are shown in Table 2.

The mean obtained FoBMO angle was −5.99 ± 3.63-degrees. The mean quality score of each RNFL and BMO-MRW was quite good at 28.73 ± 3.34 and 32.00 ± 3.17, respectively (Table 1).

TABLE 3. Comparison of Progression Rates between BMO-MRW and RNFL in Each Sector

Comparison of Coefficients by Sector (Raw Data)		
Sector	Z-score	*P* Value
G	−2.9782	**0.0029**
T	−2.1139	**0.0345**
TS	−2.7833	**0.0054**
TI	−3.6688	**0.0002**
N	−1.3483	0.1776
NS	−2.7105	**0.0067**
NI	−2.4951	**0.0126**

BMO-MRW = Bruch's membrane opening-minimum rim width; G = global; N = nasal; NI = inferonasal; NS = superonasal; RNFL = retinal nerve fiber layer; T = temporal; TI = inferotemporal; TS = superotemporal.

P values were derived by *t*-test. Values in bold face are significant *P* values ($P < 0.05$).

The ROC in the global BMO-MRW and RNFL was −3.507 ± 0.675 μm/y and −1.404 ± 0.208 μm/y, respectively (Table 2). The ROC was the greatest in the inferotemporal sector, subsequently by the superotemporal sector. The ROCs in the BMO-MRW and RNFL in the inferotemporal sector were −9.141 ± 1.254 μm/y and −4.204 ± 0.490 μm/y, respectively. The ROCs in BMO-MRW and RNFL in the superotemporal sector were 4.422 ± 1.020 μm/y and −1.353 ± 0.420 μm/y, respectively. The ROCs in the other sectors are shown in Table 2.

• **COMPARISON OF THE RATE OF CHANGE IN BMO-MRW AND RNFL:** The ROC per year was significantly different between BMO-MRW and RNFL in the global region and all Garway-Heath sectors (T = temporal; TS = superotemporal; NS = superonasal; N = nasal; NI = inferonasal; TI = inferotemporal) (*t*-test $P < .05$) but not in the nasal sector (*t*-test $P = .1776$) (Table 3). The 95% confidence interval (CI) of the ROC in BMO-MRW and RNFL from the global region, and the T, ST, IT, SN, and NI sectors did not overlap with each other, which indicates that each BMO-MRW and RNFL value was significantly different in the global region and in these sectors. However, the nasal sectors showed an overlap in the 95% CI between BMO-MRW and RNFL, including point estimates, which suggests that these 2 parameters were not significantly different in the nasal sector (Figure 2, A). Figure 2, A shows consistent findings of the comparison analysis of progression rates shown in Table 3.

A representative case demonstrating serial recurrent DHs from April 2017 to August 2019 is shown in Figure 3, A. Simple regression analysis calculating only the global region of BMO-MRW (Figure 3, B) and the RNFL (Figure 3,C) by installed software of OCT is shown. Note that the slope of BMO-MRW is −4.1 μm/y, whereas the slope of the RNFL is −2.1 μm/y. The *P* values of both slopes derived from 7 OCT tests were significant ($P = .03$ and $P < .01$, respectively).

• **COMPARISON OF THE PERCENTAGE OF REDUCTION IN THE RATE OF CHANGE OF BMO-MRW AND RNFL:** Because the baseline values of BMO-MRW and RNFL were different and the scales of BMO-MRW and RNFL were also different, the percentage of reduction in the rates of progression were compared as well. When the percentages of reduction in the ROCs were compared, the superotemporal and inferotemporal sectors showed significant differences ($P = .0127$, $P = .0069$, respectively) (Table 4). The other sectors demonstrated no significant differences between BMO-MRW and RNFL in the percentages of reduction in progression rates (all $P > .05$) (Table 4).

• **COMPARISON OF RATE OF CHANGE IN BMO-MRW AND RNFL AFTER STANDARDIZATION:** The progression rates in BMO-MRW and RNFL were also compared after standardization as these 2 parameters differed in scale and baseline values. Standardization was achieved by converting each value to a mean of 0.0 and a SD of 1.0. The standardized coefficients of the global region of BMO-MRW and the RNFL were −0.068 μm/y (95% CI: −0.093 to −0.042) and −0.090 μm/y (95% CI: −0.116 to −0.064), respectively. The standardized coefficients of the superotemporal (ST) sector of BMO-MRW and the RNFL were −0.069 μm/y (95% CI: −0.100 to −0.038) and −0.037 μm/y (95% CI: −0.060 to −0.014), respectively. The standardized coefficients of the inferotemporal (IT) sector of BMO-MRW and the RNFL were −0.125 μm/y (95% CI: −0.158 to −0.091) and −0.110 μm/y (95% CI: −0.135 to −0.085), respectively (Table 5). Detailed standardized coefficients are shown in Table 5.

The 95% CI of the standardized regression coefficient or the ROC for BMO-MRW and the RNFL from the global region and all 6 Garway-Heath sectors did overlap with each other, indicating that these 2 standardized parameters were not significantly different in any sectors or the global region (Figure 2, B). Figure 2, B compares the progression rates of the standardized BMO-MRW and RNFL, as shown in Table 5.

DISCUSSION

THE PRESENT STUDY INVESTIGATED THE ROC OF BMO-MRW in eyes showing optic DH in a single ethnic group of Asians. No such investigation has been conducted before. The ROC of the RNFL was compared to that of BMO-MRW in eyes showing DH, which has also not been reported before. It was found that BMO-MRW showed a significantly greater ROC than RNFL in the global region and 5 Garway-Heath sectors other than the nasal sector.

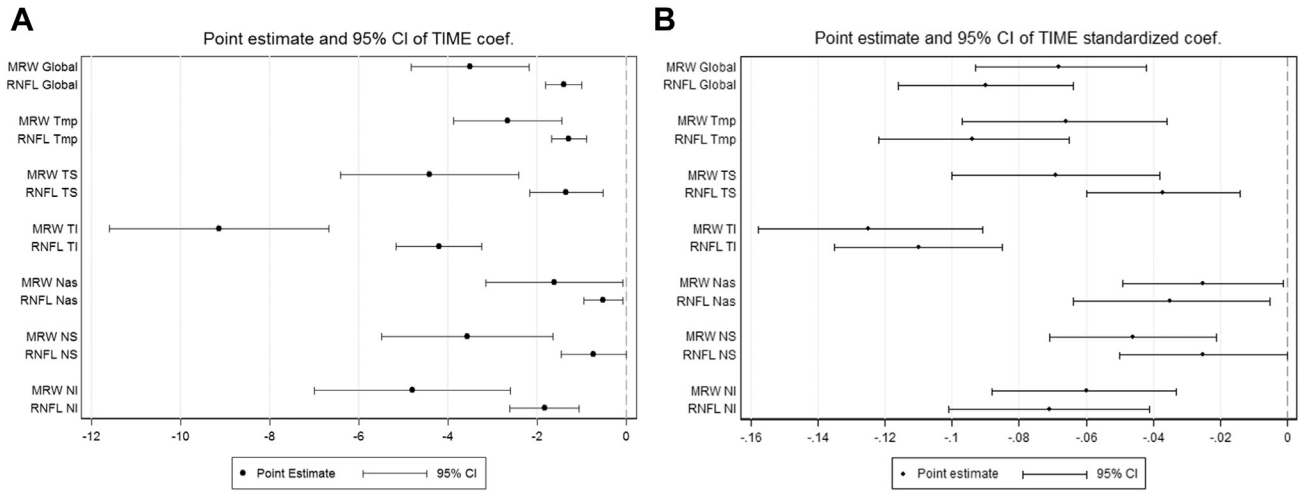

FIGURE 2. Confidence interval (CI) of each ROC for BMO-MRW and RNFL from the global region and six sectors. (A) The 95% CI of the ROC in BMO-MRW and RNFL from the global region and the Tmp, TS, TI, NS, and NI sectors, which do not overlap with each other, indicating that each BMO-MRW and RNFL value was significantly different in the global region and these sectors. However, the nasal sectors showed an overlap in 95% CI between BMO-MRW and RNFL, including point estimate, which suggests that these 2 parameters were not significantly different in the nasal sector. (B) The 95% CI of the "standardized" ROC for BMO-MRW and RNFL from the global region and all 6 Garway-Heath sectors do overlap with each other, indicating that these 2 standardized parameters are not significantly different in all sectors and the global region. The rates of change of BMO-MRW and RNFL were compared after standardization as these 2 parameters differ in scale and baseline values. BMO-MRW = Bruch's membrane opening-minimum rim width; Nas = nasal; NS = superonasal; NI = inferonasal; RNFL = retinal nerve fiber layer; ROC = rate of change; TI = inferotemporal; Tmp = temporal; TS = superotemporal.

Moreover, the percentage of ROC reduction was significantly greater for BMO-MRW than for RNFL in the IT and ST sectors. However, when these 2 parameters were compared after standardization, they did not show significant differences in the global region or any of the 6 sectors.

The ROC in BMO-MRW and RNFL was studied in Canada to investigate the effects of normal aging.[38] Given the study location, mainly whites were included. In healthy subjects, the BMO-MRW ROC was −1.92 mm/year ($P < .01$) and that of RNFL was −0.44 mm/year ($P = .01$). The global ROC in eyes showing DH was −3.507 ± 0.675 μm/y ($P < .0001$) for BMO-MRW and −1.404 ± 0.208 μm/y ($P < .0001$) for RNFL in the present study consisting mainly of glaucoma patients (92.7%). The rates of deterioration of BMO-MRW and the RNFL were faster in eyes showing DH in the present study than in the normal aging investigated in the previous study.[38] However, the previous study did not compare the BMO-MRW and RNFL parameters, nor were they compared in Asians. Considering the different ethnicity included in the previous study, direct comparison with the current study results is difficult, but it could still provide relevant ROCs.

Another study by Bowd and associates[39] reported that the ROC in BMO-MRW was −1.82 mm/year and −2.20 mm/y in eyes with suspected glaucoma in the study of populations descended from Europeans and Africans, respectively, which was significantly different ($P = .03$). The ROC of RNFL was −0.64 mm/y and −0.75 mm/y in eyes suspected of glaucoma in European and African descendants, respectively ($P = .75$). No ethnicity-associated differences in ROC were found in healthy controls or glaucoma subjects.[39] In glaucoma eyes, the ROC of BMO-MRW was −2.87 mm/y and −2.91 mm/y in European and African descendants, respectively ($P = .21$). The ROC of the RNFL was −0.94 mm/y and −0.89 mm/y in glaucoma eyes in populations of European and African descendants, respectively ($P = .40$). In the current study, the mean rates of reduction in BMO-MRW (−3.507 ± 0.675 μm/y) and RNFL (−1.404 ± 0.208 μm/y) were faster in eyes showing DH than in eyes examined in the previous study by Bowd and associates.[39] However, that study did not investigate the ROC in structural tests in Asians, and direct comparison with the present study may not be correct, but the data suggest faster progression in eyes showing DH.

Baseline BMO-MRW and RNFL thicknesses were reported to significantly affect each ROC, with higher baseline values associated with faster deterioration.[38] The mean baseline global BMO-MRW was 203.04 ± 57.97 μm, and the mean global RNFL was 82.88 ± 15.37 μm in the present study. Notably, the baseline BMO-MRW was much greater than that of the RNFL, and the ROC was also greater for BMO-MRW than for RNFL in the present study, which was consistent with previous studies, although these 2 parameters were not compared statistically in other studies. Because BMO-MRW and RNFL have different

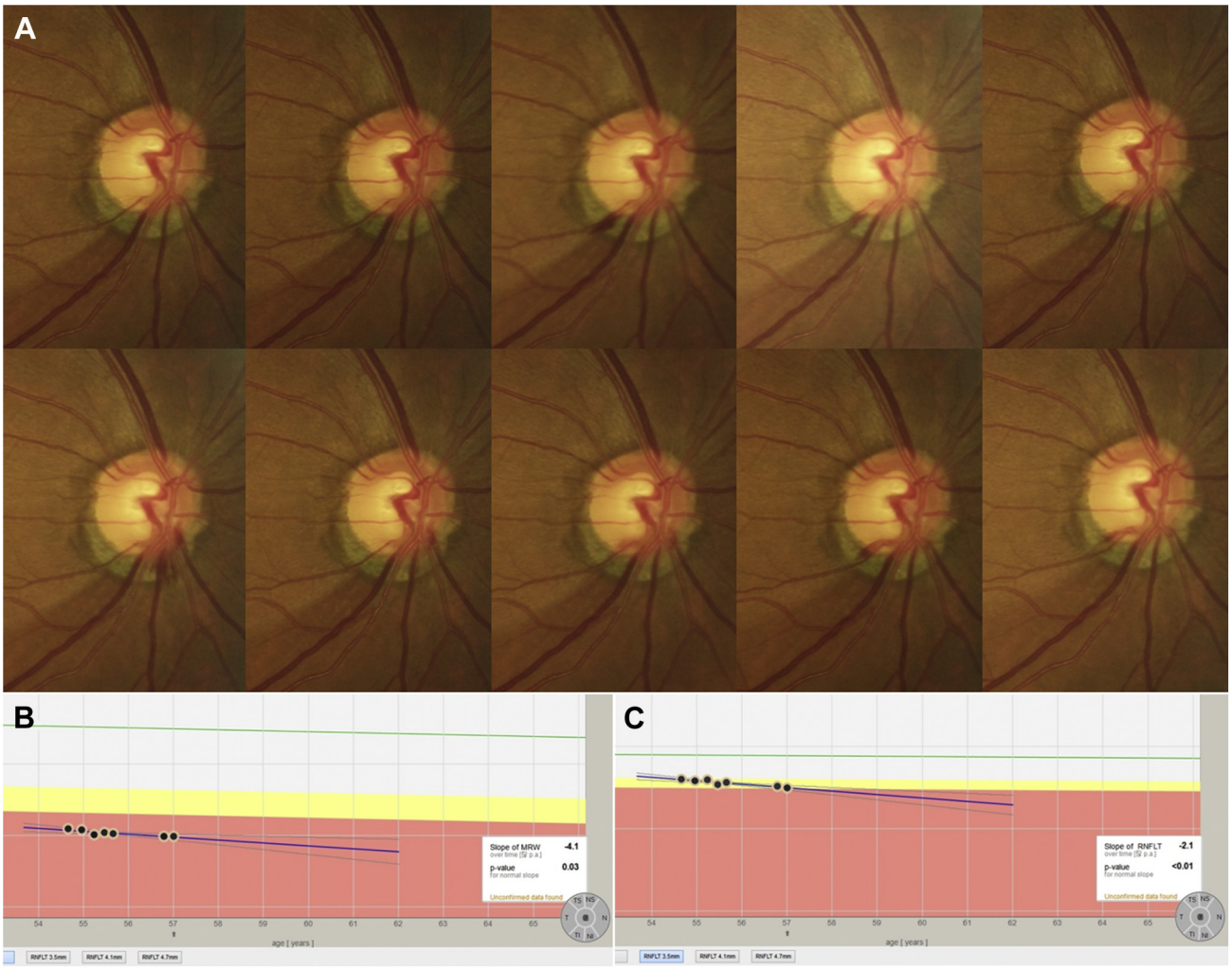

FIGURE 3. (A) Representative case shows serial optic disc hemorrhage and serially recurrent DH from April 2017 to August 2019. Simple regression analysis was used to calculate only the global region of BMO-MRW (B) and the RNFL (C) using commercial software. Note the BMO-MRW slope is −4.1 μm/y, whereas the slope of the RNFL is −2.1 μm/y. The *P* values of both slopes from 7 OCT tests are significant ($P = .03$ and $P < .01$, respectively). Baseline data without DH were included for reference to eliminate the potential effect or bias of initial DHs on OCT parameters in calculating longitudinal rates of change. BMO-MRW = Bruch's membrane opening-minimum rim width; DH = disc hemorrhage; OCT = optical coherence tomography; RNFL = retinal nerve fiber layer.

baseline values and different scales, with BMO-MRW showing higher values than RNFL, the ROC in BMO-MRW may be greater than that of the RNFL. However, in eyes prone to slow progression or normal aging, the actual differences in values may be small, as shown in previous studies. Moreover, the progression rates between BMO-MRW and RNFL may not be statistically different, although there were no direct comparisons in previous studies.[38,39] DH has been widely shown to be associated with faster glaucomatous progression than in those without DH.[2,3,7,8,11,13–19] Therefore, when the rate of deterioration is greater in subjects with DH, the difference in the rate of progression between the 2 parameters of BMO-MRW and the RNFL may also be greater than for those without DH. This point partially explains the greater ROC in BMO-MRW than in the RNFL in all sectors, except for the nasal sector in the present study with eyes showing DH. The nasal sector is known to be a relatively less active sector of glaucomatous change than the temporal sectors.[39,40]

Both the intra- and the interobserver reproducibility of BMO-MRW have been previously reported to be excellent.[37,41,42] Although the actual value and scale of BMO-MRW are greater than those of RNFL, this does not necessarily mean that the BMO-MRW values are more variable than the RNFL. As shown in previous studies, BMO-MRW provided excellent reproducibility and repeatability, comparable to those of the RNFL.[41,43] Therefore, BMO-

TABLE 4. Comparison of % of Reduction in Progression Rates between BMO-MRW and RNFL

Coefficients by Sector (% Reduction)				
Sector	Percent Coefficient, BMO-MRW	Percent Coefficient, RNFL	Z-score	*P* Value
G	−1.6952 ± 0.3263	−1.3844 ± 0.2046	−0.8069	0.4197
T	−1.7985 ± 0.4181	−1.8308 ± 0.2811	0.0642	0.9488
TS	−2.5445 ± 0.5868	−0.9192 ± 0.2851	−2.4913	**0.0127**
TI	−6.0908 ± 0.8353	−3.5682 ± 0.4155	−2.7040	**0.0069**
N	−0.6000 ± 0.2914	−0.6043 ± 0.2603	0.0111	0.9911
NS	−1.2447 ± 0.3409	−0.5486 ± 0.2804	−1.5771	0.1148
NI	−2.0948 ± 0.4892	−1.4407 ± 0.3085	−1.1311	0.2580

BMO-MRW = Bruch membrane opening-minimum rim width; G = global; N = nasal; NI = inferonasal; NS = superonasal; RNFL = retinal nerve fiber layer; T = temporal; TI = inferotemporal; TS = superotemporal.

P values were derived by *t*-test. Bold values indicate significant *P* values ($P < 0.05$).

TABLE 5. Progression Rate of BMO-MRW and RNFL After Standardization

		95% CI	
Outcome	Standardized Coefficient	Lower	Upper
BMO-MRW Global	−0.068	−0.093	−0.042
RNFL Global	−0.090	−0.116	−0.064
BMO-MRW T	−0.066	−0.097	−0.036
RNFL T	−0.094	−0.122	−0.065
BMO-MRW TS	−0.069	−0.100	−0.038
RNFL TS	−0.037	−0.060	−0.014
BMO-MRW TI	−0.125	−0.158	−0.091
RNFL TI	−0.110	−0.135	−0.085
BMO-MRW N	−0.025	−0.049	−0.001
RNFL N	−0.035	−0.064	−0.005
BMO-MRW NS	−0.046	−0.071	−0.021
RNFL NS	−0.025	−0.050	0.000
BMO-MRW NI	−0.060	−0.088	−0.033
RNFL NI	−0.071	−0.101	−0.041

BMO-MRW = Bruch's membrane opening-minimum rim width; CI = confidence interval; G = global; N = nasal; NI = inferonasal; NS = superonasal; RNFL = retinal nerve fiber layer; T = temporal; TI = inferotemporal; TS = superotemporal.

Generalized linear mixed-model including random intercept for subjects after standardization.

MRW may be more beneficial for detecting significant changes than RNFL because BMO-MRW can show visible reductions in the deterioration better than RNFL, especially in the case of rapid progression, such as in eyes with DH.

The IT sector showed the greatest ROC, followed by the ST sector in both BMO-MRW and RNFL in the present study. Moreover, the IT and ST sectors showed significant differences in the percentage of reduction between BMO-MRW and RNFL. It has been reported that DH in the ST and IT sectors showed more successive structural and functional change than in the temporal and nasal sectors.[40] In addition, Bowd and associates found that the location of change was mainly temporal and inferior in all diagnostic groups for BMO-MRW.[39] DHs are most frequently detected in the IT sector along with the ST sector and are least identified in the nasal sector.[13,14,44,45] Among these regions, the IT and ST sectors are also the regions where early glaucomatous alterations are most commonly observed.[46,47] DH is prone to occur in regions where the active site of glaucomatous damage happens. DH was first regarded as an antecedent for glaucomatous injury since the discovery of DH was subsequently accompanied by a glaucoma diagnosis or progression.[2,3,7,8,11,13,14,16–19] However, recently, it has been proposed that DH may not be a distinct occasion resulting in deterioration but rather a consequence of glaucomatous alterations.[2,4,20,21]

The pathogenesis of DH remains unclear. There are several hypotheses concerning DH, including mechanical and ischemic theories. Recently, a novel hypothesis regarding the pathogenesis of DH has been proposed.[2] For the frequently observed splinter-shaped peripapillary hemorrhage, reactive gliosis has been proposed to be related to the pathogenesis of DH. Proliferative reactive gliosis results in the production of fibrous glial scars, which generate a traction force that may disrupt a capillary at the boundary between the healthy normal and injured RNFL and, thus, develop a splinter-shaped peripapillary DH. Besides glial scar production, the remodeling and distortion of beams of the lamina cribrosa could injure the capillary structure in vicinity to the lamina cribrosa pores, resulting in the formation of round blot-shaped cup hemorrhage, which is a less frequently observed form of DH than splinter DH.[2]

BMO is the external edge of the NRR tissue at the optic disc and RGC axons pass through BMO.[23,24,48] BMO-MRW has been demonstrated to have the benefit of correctly reflecting the amount of optic disc neural tissue.[22,27,28,49] Partly because the scale of BMO-MRW is

greater than that of the RNFL and also because eyes with DH have a faster ROC than those without DH, BMO-MRW revealed a significantly faster ROC than that of RNFL in subjects exhibiting DH. It is surprising that when these 2 parameters were standardized, there were no significant differences between the ROC of the BMO-MRW and that of the RNFL. However, it is still more advantageous to use BMO-MRW to detect early progression in eyes showing DH than to use changes in the RNFL, because the actual values show a greater progression rate. Because DH happens directly at the optic disc and not at the peripapillary region, BMO-MRW may also reflect the changes better than the RNFL measured at the peripapillary area. Considering the clinical importance of DH, which is more prone to glaucomatous progression, BMO-MRW offers a visible ROC to benefit the detection of early deterioration. These findings suggest that even when the RNFL shows no significant ROC, BMO-MRW can show a significant rate of deterioration. In these eyes showing DH, clinicians may consider enhancing the treatment intensity or having more frequent follow-ups.

A study that evaluated the rate of 3-dimensional NRR thinning (3D-NRT) in glaucoma subjects with DH reported that DH eyes showed a relatively faster thinning of the average RNFL thickness than the 3D-NRT after normalization, especially in the IT region.[50] 3D-NRT was indicated by the distance between the BMO and vitreoretinal interface in their study. 3D-NRT was obtained by using Cirrus OCT (Zeiss, Jena, Switzerland), whereas BMO-MRW was obtained by using the Spectralis OCT (Heidelberg Engineering). They both evaluate NRR, but the methods are not exactly the same. The discrepancy between the methods of rim parameters from different OCT devices may have caused the disagreement with the results our study. However, the previous study also found that the IT region (7-o'clock location) showed a faster ROC than other clock-hour locations, which is consistent with the present results. Cirrus OCT analyzes the optic disc regions in simple clock-hour locations, whereas Spectralis OCT analyzes the disc regions in Garway-Heath sectors with individual cyclotorsion adjusted with the FoBMO axis, which provides a more accurate sectoral analysis of the optic disc.

The majority of diagnoses in the subjects (69.5%) in this study were NTG. In Asian populations, NTG consists mostly (76.3%) of open-angle glaucoma, as investigated in population-based studies in Asians.[51] DH was reported more often in NTG than in other types of glaucoma, ranging from 2.9% to 31.3%.[52–56] Therefore, in the present study conducted in a single ethnic group of Asians, NTG was mainly included with a normative range of baseline intraocular pressure (14.82 ± 3.21 mm Hg). The spherical equivalent of the included subjects showed near emmetropia, at −1.77 ± 2.53 D. The effect of potential myopia may have been excluded from the present study. The glaucoma stage of the included subjects showed early glaucoma based on a mean deviation of −4.41 ± 5.04 dB. DHs are reported to be more frequently observed in the early and moderate stages of glaucoma and are observed much less in the advanced stages.[7,52,53,57] In this regard, the subjects included in the current study with DH revealed an early stage of glaucoma. Moreover, an early stage of glaucoma shows relatively greater changes in structural tests compared to the small changes in functional tests.[32–34] Therefore, it is more beneficial to use structural parameters, for example, BMO-MRW, in detection of early glaucomatous deterioration in eyes showing DH with early glaucoma.

There were several limitations to the current study. One possible limitation was its retrospective nature. Only subjects who had had both RNFL and BMO-MRW analyses more than 5 times and who had a reliable quality of both structural tests were included. The effect of including such subjects in results is not known. Second, it was a hospital-based design performed at a referral university hospital of the province and not a population-based study. The included subjects might not have represented the entire normal population. Third, the relatively small sample size of this study should also be considered, although its longitudinal design limited wide inclusion. Moreover, the follow-up period was not very long, although it was 21.57 ± 7.88 months with 7.88 ± 2.39 OCT tests. However, having 82 subjects included in the study with a follow-up period of nearly 2 years may be enough to reveal the trend in the ROC in a single condition showing DH in glaucoma spectrum eyes. A large multicenter study with long-term follow-up is needed. And last, DH might have been missed on disc photography between the clinic visits or even before the initial visits, as reported in previous studies.[58–60] Because exact time the DHs were initiated was not known, patients were enrolled when a DH was detected at least once in the authors' clinic in observations conducted every 3 months. In this regard, we did not investigate the factors relating to the recurrence of DH, because single-occurrence DH may also be recurrent DH missed between visits. However, quite a proportion of the subjects showed recurrent DHs, and many showed DHs at multiple locations, even at both the inferior and superior hemifields. Therefore, we did not define the initial location of the DHs or investigate the factors associated with the initial location of the DHs. However, our results showed that the active and susceptible sites of glaucomatous injury, such as the IT and ST sectors, had a faster ROCs than did other regions, such as the nasal sector.

In conclusion, this study found that BMO-MRW showed a significantly greater ROC than RNFL in eyes showing DH, which are prone to glaucomatous progression. The ROC was the greatest in the IT sector and subsequently in the ST sector in both BMO-MRW and the RNFL, and the nasal sector showed no significant differences between the ROC in BMO-MRW and that in the RNFL. The percentage of reduction in the ROC was significantly greater

in the BMO-MRW than in the RNFL, especially in the IT and ST sectors. No such study demonstrating the longitudinal ROC of BMO-MRW compared to RNFL in a single ethnic group of Asians (Koreans), particularly in subjects with DH has been reported before. Our results suggest that the new parameter, BMO-MRW, may be more beneficial for detecting glaucomatous progression earlier than changes in RNFL in eyes showing DH, which are more likely to progress, and is, therefore, of clinical importance. Clinicians should consider intensifying the treatment strategy according to the ROC, especially in cases suggesting fast progression based on BMO-MRW. A large, population-based study is needed in the future to draw more definitive conclusions.

ALL AUTHORS HAVE COMPLETED AND SUBMITTED THE ICMJE FORM FOR DISCLOSURE OF POTENTIAL CONFLICTS OF INTEREST and none were reported.

Funding/Support: This study received no financial support.

Financial Disclosures: The authors have reported that they have no relationships relevant to the contents of this paper to disclose.

REFERENCES

1. Weinreb RN, Khaw PT. Primary open-angle glaucoma. *Lancet* 2004;363:1711–1720.
2. Lee EJ, Han JC, Kee C. A novel hypothesis for the pathogenesis of glaucomatous disc hemorrhage. *Prog Retin Eye Res* 2017;60:20–43.
3. Bengtsson B. Optic disc haemorrhages preceding manifest glaucoma. *Acta Ophthalmol (Copenh)* 1990;68:450–454.
4. Chung E, Demetriades AM, Christos PJ, Radcliffe NM. Structural glaucomatous progression before and after occurrence of an optic disc haemorrhage. *Br J Ophthalmol* 2015;99:21–25.
5. De Moraes CG, Liebmann JM, Park SC, et al. Optic disc progression and rates of visual field change in treated glaucoma. *Acta Ophthalmol* 2013;91:e86–e91.
6. De Moraes CG, Prata TS, Liebmann CA, Tello C, Ritch R, Liebmann JM. Spatially consistent, localized visual field loss before and after disc hemorrhage. *Invest Ophthalmol Vis Sci* 2009;50:4727–4733.
7. Diehl DL, Quigley HA, Miller NR, Sommer A, Burney EN. Prevalence and significance of optic disc hemorrhage in a longitudinal study of glaucoma. *Arch Ophthalmol* 1990;108:545–550.
8. Drance SM, Fairclough M, Butler DM, Kottler MS. The importance of disc hemorrhage in the prognosis of chronic open angle glaucoma. *Arch Ophthalmol* 1977;95:226–228.
9. Drance SM. Disc hemorrhages in the glaucomas. *Surv Ophthalmol* 1989;33:331–337.
10. Ernest PJ, Schouten JS, Beckers HJ, Hendrikse F, Prins MH, Webers CA. An evidence-based review of prognostic factors for glaucomatous visual field progression. *Ophthalmology* 2013;120:512–519.
11. Ishida K, Yamamoto T, Sugiyama K, Kitazawa Y. Disk hemorrhage is a significantly negative prognostic factor in normal-tension glaucoma. *Am J Ophthalmol* 2000;129:707–714.
12. Siegner SW, Netland PA. Optic disc hemorrhages and progression of glaucoma. *Ophthalmology* 1996;103:1014–1024.
13. Sonnsjo B, Dokmo Y, Krakau T. Disc haemorrhages, precursors of open angle glaucoma. *Prog Retin Eye Res* 2002;21:35–56.
14. Healey PR, Mitchell P, Smith W, Wang JJ. Optic disc hemorrhages in a population with and without signs of glaucoma. *Ophthalmology* 1998;105:216–223.
15. Drance S, Anderson DR, Schulzer M, for the Collaborative Normal-Tension Glaucoma Study Group. Risk factors for progression of visual field abnormalities in normal-tension glaucoma. *Am J Ophthalmol* 2001;131:699–708.
16. Budenz DL, Anderson DR, Feuer WJ, et al. Detection and prognostic significance of optic disc hemorrhages during the Ocular Hypertension Treatment Study. *Ophthalmology* 2006;113:2137–2143.
17. Drance SM, Begg IS. Sector haemorrhage–a probable acute ischaemic disc change in chronic simple glaucoma. *Can J Ophthalmol* 1970;5:137–141.
18. Shihab ZM, Lee PF, Hay P. The significance of disc hemorrhage in open-angle glaucoma. *Ophthalmology* 1982;89:211–213.
19. Tuulonen A, Takamoto T, Wu DC, Schwartz B. Optic disk cupping and pallor measurements of patients with a disk hemorrhage. *Am J Ophthalmol* 1987;103:505–511.
20. Gracitelli CP, Tatham AJ, Zangwill LM, Weinreb RN, Liu T, Medeiros FA. Estimated rates of retinal ganglion cell loss in glaucomatous eyes with and without optic disc hemorrhages. *PLoS One* 2014;9:e105611.
21. Park HY, Kim EK, Park CK. Clinical significance of the location of recurrent optic disc hemorrhage in glaucoma. *Invest Ophthalmol Vis Sci* 2015;56:7524–7534.
22. Chauhan BC, Burgoyne CF. From clinical examination of the optic disc to clinical assessment of the optic nerve head: a paradigm change. *Am J Ophthalmol* 2013;156:218–227.
23. Chen TC. Spectral domain optical coherence tomography in glaucoma: qualitative and quantitative analysis of the optic nerve head and retinal nerve fiber layer (an AOS thesis). *Trans Am Ophthalmol Soc* 2009;107:254–281.
24. Povazay B, Hofer B, Hermann B, et al. Minimum distance mapping using three-dimensional optical coherence tomography for glaucoma diagnosis. *J Biomed Opt* 2007;12:41204.
25. Reis AS, O'Leary N, Yang H, et al. Influence of clinically invisible, but optical coherence tomography detected, optic disc margin anatomy on neuroretinal rim evaluation. *Invest Ophthalmol Vis Sci* 2012;53:1852–1860.
26. Strouthidis NG, Fortune B, Yang H, Sigal IA, Burgoyne CF. Longitudinal change detected by spectral domain optical coherence tomography in the optic nerve head and peripapillary retina in experimental glaucoma. *Invest Ophthalmol Vis Sci* 2011;52:1206–1219.
27. Chauhan BC, Danthurebandara VM, Sharpe GP, et al. Bruch's membrane opening minimum rim width and retinal nerve fiber layer thickness in a normal white population: a multicenter study. *Ophthalmology* 2015;122:1786–1794.

28. Chauhan BC, O'Leary N, AlMobarak FA, et al. Enhanced detection of open-angle glaucoma with an anatomically accurate optical coherence tomography-derived neuroretinal rim parameter. *Ophthalmology* 2013;120:535–543.
29. Mizumoto K, Gosho M, Zako M. Correlation between optic nerve head structural parameters and glaucomatous visual field indices. *Clin Ophthalmol* 2014;8:1203–1208.
30. Pollet-Villard F, Chiquet C, Romanet JP, Noel C, Aptel F. Structure-function relationships with spectral-domain optical coherence tomography retinal nerve fiber layer and optic nerve head measurements. *Invest Ophthalmol Vis Sci* 2014;55:2953–2962.
31. Gardiner SK, Ren R, Yang H, Fortune B, Burgoyne CF, Demirel S. A method to estimate the amount of neuroretinal rim tissue in glaucoma: comparison with current methods for measuring rim area. *Am J Ophthalmol* 2014;157:540–549.
32. Malik R, Swanson WH, Garway-Heath DF. 'Structure-function relationship' in glaucoma: past thinking and current concepts. *Clin Exp Ophthalmol* 2012;40:369–380.
33. Keltner JL, Johnson CA, Anderson DR, et al. The association between glaucomatous visual fields and optic nerve head features in the Ocular Hypertension Treatment Study. *Ophthalmology* 2006;113:1603–1612.
34. Hood DC, Kardon RH. A framework for comparing structural and functional measures of glaucomatous damage. *Prog Retin Eye Res* 2007;26:688–710.
35. Enders P, Schaub F, Adler W, et al. Bruch's membrane opening-based optical coherence tomography of the optic nerve head: a useful diagnostic tool to detect glaucoma in macrodiscs. *Eye (Lond)* 2018;32:314–323.
36. Lopes FS, Matsubara I, Almeida I, et al. Structure-function relationships in glaucoma using enhanced depth imaging optical coherence tomography-derived parameters: a cross-sectional observational study. *BMC Ophthalmol* 2019;19:52.
37. Cho HK, Kee C. Characteristics of patients showing discrepancy between bruch's membrane opening-minimum rim width and peripapillary retinal nerve fiber layer thickness. *J Clin Med* 2019;8:1362.
38. Vianna JR, Danthurebandara VM, Sharpe GP, et al. Importance of normal aging in estimating the rate of glaucomatous neuroretinal rim and retinal nerve fiber layer loss. *Ophthalmology* 2015;122:2392–2398.
39. Bowd C, Zangwill LM, Weinreb RN, et al. Racial differences in rate of change of spectral-domain optical coherence tomography-measured minimum rim width and retinal nerve fiber layer thickness. *Am J Ophthalmol* 2018;196:154–164.
40. Hsia Y, Su CC, Wang TH, Huang JY. Clinical characteristics of glaucoma patients with disc hemorrhage in different locations. *Graefes Arch Clin Exp Ophthalmol* 2019;257:1955–1962.
41. Reis ASC, Zangalli CES, Abe RY, et al. Intra- and interobserver reproducibility of Bruch's membrane opening minimum rim width measurements with spectral domain optical coherence tomography. *Acta Ophthalmol* 2017;95:e548–e555.
42. Park K, Kim J, Lee J. Reproducibility of Bruch membrane opening-minimum rim width measurements with spectral domain optical coherence tomography. *J Glaucoma* 2017;26:1041–1050.
43. Enders P, Bremen A, Schaub F, et al. Intraday repeatability of bruch's membrane opening-based neuroretinal rim measurements. *Invest Ophthalmol Vis Sci* 2017;58:5195–5200.
44. Kim YK, Park KH, Yoo BW, Kim HC. Topographic characteristics of optic disc hemorrhage in primary open-angle glaucoma. *Invest Ophthalmol Vis Sci* 2014;55:169–176.
45. Ozturker ZK, Munro K, Gupta N. Optic disc hemorrhages in glaucoma and common clinical features. *Can J Ophthalmol* 2017;52:583–591.
46. Akagi T, Zangwill LM, Saunders LJ, et al. Rates of local retinal nerve fiber layer thinning before and after disc hemorrhage in glaucoma. *Ophthalmology* 2017;124:1403–1411.
47. Kotowski J, Wollstein G, Ishikawa H, Schuman JS. Imaging of the optic nerve and retinal nerve fiber layer: an essential part of glaucoma diagnosis and monitoring. *Surv Ophthalmol* 2014;59:458–467.
48. Suh MH, Park KH, Kim H, et al. Glaucoma progression after the first-detected optic disc hemorrhage by optical coherence tomography. *J Glaucoma* 2012;21:358–366.
49. Toshev AP, Lamparter J, Pfeiffer N, Hoffmann EM. Bruch's membrane opening-minimum rim width assessment with spectral-domain optical coherence tomography performs better than confocal scanning laser ophthalmoscopy in discriminating early glaucoma patients from control subjects. *J Glaucoma* 2017;26:27–33.
50. Kim YW, Lee WJ, Seol BR, Kim YK, Jeoung JW, Park KH. Rate of three-dimensional neuroretinal rim thinning in glaucomatous eyes with optic disc haemorrhage. *Br J Ophthalmol* 2020;104(5):648–654.
51. Cho HK, Kee C. Population-based glaucoma prevalence studies in Asians. *Surv Ophthalmol* 2014;59:434–447.
52. Kitazawa Y, Shirato S, Yamamoto T. Optic disc hemorrhage in low-tension glaucoma. *Ophthalmology* 1986;93:853–857.
53. Jonas JB, Xu L. Optic disk hemorrhages in glaucoma. *Am J Ophthalmol* 1994;118:1–8.
54. Kim DW, Kim YK, Jeoung JW, Kim DM, Park KH. for the Epidemiologic Survey Committee of the Korean Ophthalmological S. Prevalence of optic disc hemorrhage in Korea: the Korea National Health and Nutrition Examination Survey. *Invest Ophthalmol Vis Sci* 2015;56:3666–3672.
55. Gloster J. Incidence of optic disc haemorrhages in chronic simple glaucoma and ocular hypertension. *Br J Ophthalmol* 1981;65:452–456.
56. Hendrickx KH, van den Enden A, Rasker MT, Hoyng PF. Cumulative incidence of patients with disc hemorrhages in glaucoma and the effect of therapy. *Ophthalmology* 1994;101:1165–1172.
57. Yamamoto T, Iwase A, Kawase K, Sawada A, Ishida K. Optic disc hemorrhages detected in a large-scale eye disease screening project. *J Glaucoma* 2004;13:356–360.
58. de Beaufort HC, De Moraes CG, Teng CC, et al. Recurrent disc hemorrhage does not increase the rate of visual field progression. *Graefes Arch Clin Exp Ophthalmol* 2010;248:839–844.
59. Kim SH, Park KH. The relationship between recurrent optic disc hemorrhage and glaucoma progression. *Ophthalmology* 2006;113:598–602.
60. Nitta K, Sugiyama K, Higashide T, Ohkubo S, Tanahashi T, Kitazawa Y. Does the enlargement of retinal nerve fiber layer defects relate to disc hemorrhage or progressive visual field loss in normal-tension glaucoma? *J Glaucoma* 2011;20:189–195.